

Polyglycerol-Functionalized β -Cyclodextrins as Crosslinkers in Thermoresponsive Nanogels for the Enhanced Dermal Penetration of Hydrophobic Drugs

Huiyi Wang, Neha Tiwari, Maria Soledad Orellano, Lucila Navarro, Zahra Beiranvand, Mohsen Adeli, and Marcelo Calderón*

Thermoresponsive nanogels (tNGs) are promising candidates for dermal drug delivery. However, poor incorporation of hydrophobic drugs into hydrophilic tNGs limits the therapeutic efficiency. To address this challenge, β -cyclodextrins (β -CD) are functionalized by hyperbranched polyglycerol serving as crosslinkers (hPG- β CD) to fabricate β CD-tNGs. This novel construct exhibits augmented encapsulation of hydrophobic drugs, shows the appropriate thermal response to dermal administration, and enhances the dermal penetration of payloads. The structural influences on the encapsulation capacity of β CD-tNGs for hydrophobic drugs are analyzed, while concurrently retaining their efficacy as skin penetration enhancers. Various synthetic parameters are considered, encompassing the acrylation degree and molecular weight of hPG- β CD, as well as the monomer composition of β CD-tNGs. The outcome reveals that β CD-tNGs substantially enhance the aqueous solubility of Nile Red elevating to $120 \mu\text{g mL}^{-1}$ and augmenting its dermal penetration up to $3.33 \mu\text{g cm}^{-2}$. Notably, the acrylation degree of hPG- β CD plays a significant role in dermal drug penetration, primarily attributed to the impact on the rigidity and hydrophilicity of β CD-tNGs. Taken together, the introduction of the functionalized β -CD as the crosslinker in tNGs presents a novel avenue to enhance the efficacy of hydrophobic drugs in dermatological applications, thereby offering promising opportunities for boosted therapeutic outcomes.

1. Introduction

Over the last decades, topical drug delivery has been under the spotlight of the medical research field.^[1] In contrast to systemic strategies, such as oral delivery, intravenous injection, and intranasal inhalation, topical drug delivery offers higher therapeutic efficacy and convenience. It allows localized and non-invasive drug delivery, which minimizes the systemic risk from side effects and optimizes patient compliance.^[2] Skin drug delivery is a popular topical administration, which can decrease therapeutic action time and enhance efficacy by avoiding blood circulation and first-pass metabolism.^[3] However, as the body armor, the skin plays an essential role in protecting the body from external environmental insults, like UV irradiation, mechanical harm, penetration of hazardous substances, etc. Therein, the stratum corneum (SC) is the outermost barrier for preventing the permeation of drug molecules.^[4] To leap over the defensive barrier imposed by the SC, nanotechnology is a promising strategy.^[5,6] Nanocarriers such as micelles,^[7,8] nanogels

H. Wang, N. Tiwari, M. S. Orellano, M. Calderón
POLYMAT, Applied Chemistry Department
Faculty of Chemistry
University of the Basque Country, UPV/EHU
Donostia-San Sebastian 20018, Spain
E-mail: marcelo.calderon@ehu.eus

L. Navarro
Instituto de Desarrollo Tecnológico para la Industria Química (INTEC),
Consejo Nacional de Investigaciones Científicas y Técnicas (CONICET)
Universidad Nacional del Litoral (UNL)
Santa Fe 3000, Argentina
Z. Beiranvand, M. Adeli
Department of Chemistry
Faculty of Science
Lorestan University
Khorramabad 68151-44316, Iran
M. Calderón
IKERBASQUE
Basque Foundation for Science
Bilbao 48009, Spain

 The ORCID identification number(s) for the author(s) of this article can be found under <https://doi.org/10.1002/smll.202311166>

© 2024 The Authors. Small published by Wiley-VCH GmbH. This is an open access article under the terms of the [Creative Commons Attribution-NonCommercial](https://creativecommons.org/licenses/by-nc/4.0/) License, which permits use, distribution and reproduction in any medium, provided the original work is properly cited and is not used for commercial purposes.

DOI: 10.1002/smll.202311166

(NGs),^[9–11] liposomes,^[12,13] and inorganic nanoparticles,^[14,15] have been proven to deliver therapeutic molecules into the skin, showing high dermal permeation, as well as improved stability and biocompatibility.^[16,17] Furthermore, they can be tuned to achieve controllable drug release. These benefits optimize the accuracy and pharmacokinetics of therapeutics.^[18]

NGs are good candidates for topical drug delivery, due to their soft crosslinked network of polymeric chains in the nanoscale range and high water content.^[19] They can effectively load various therapeutics, such as proteins, small drug molecules, and dyes. To release the cargo in a controllable manner inside the skin tissue, thermoresponsive NGs (tNGs) with a cloud point temperature (T_{cp}) in the range of 32–37 °C are designed, which allows the spontaneous release of cargoes with the trigger of the natural skin temperature gradient.^[20,21] When the body temperature exceeds their T_{cp} , tNGs undergo volume shrinkage, extruding the loaded cargoes to achieve the specific drug release.^[11,22] Apart from these intrinsic benefits, tNGs can cause a hydration effect on the skin, which reversibly disrupts the SC structure to boost the delivery of therapeutics into deeper skin layers.^[23] It has been demonstrated that the skin hydration effect is important for enhancing skin permeability and increasing drug absorption and retention.^[24]

NGs are ideal nanocarriers for delivering hydrophilic molecules into skin tissue.^[25,26] Whereas, poor encapsulation of hydrophobic molecules into hydrophilic NGs still restrains therapeutic efficiency. To address this hurdle, cyclodextrin (CD), approved for drug delivery by the Food and Drug Administration of the USA (FDA), has caught researchers' attention.^[27] CD owns an amphiphilic toroid structure of a hydrophobic interior cavity and a hydrophilic exterior surface.^[28] This unique structure makes it promising to be incorporated into hydrophilic nanocarriers for enhancing their encapsulation capacity of hydrophobic drugs.^[29,30] Moreover, CD is a popular cutaneous penetration enhancer.^[31] It can decrease the barrier function of the lipophilic membrane by extracting lipids from the skin,^[32] thereby enhancing the skin permeability.^[33] In a previous study, tNGs with β -CD attached to their surface have shown enhanced delivery efficacy of dexamethasone, particularly to the dermis layer. An effective down-regulation of the proinflammatory thymic stromal lymphopoietin expression was demonstrated, outperforming the activity of dexamethasone delivered by a commercial formulation.^[34] However, the amount of conjugated CD on the surface of the tNG was limited due to solubility issues. Accordingly, the encapsulation capacity of hydrophobic drugs and the enhancement of skin permeation were restricted. To mitigate the adverse effects associated with CD conjugation, hydrophilic polymers were chosen for the surface functionalization of nanoparticles (NPs), resulting in enhanced stability.^[35,36]

In this study, poly(*N*-isopropylacrylamide) (pNIPAM)-based tNGs were crosslinked by functionalized β -CD, aiming to improve the dermal penetration of hydrophobic drugs in a controllable manner. Given the facility in synthesis and functionalization, hyperbranched polyglycerol (hPG) was used to functionalize β -CD to fabricate the hydrophilic macromolecular crosslinker, hPG- β CD. Meanwhile, hPG can introduce good biocompatibility, minimal organ accumulation, and potential protein resistance.^[37,38] An armory of tNGs was fabricated with various molecular weights and acrylation degrees of hPG- β CD, as

well as various compositions of monomers, to study their effect more comprehensively on dermal drug delivery (Scheme 1). Nile Red (NR) was chosen as the model hydrophobic cargo due to its high stability and fluorescence properties. A quantitative *ex-vivoskin* penetration assay revealed that the β CD-tNGs showed a higher drug penetration compared to β -CD, tNGs, and the physical combinations thereof. The findings demonstrated that careful engineering of the crosslinkers in their sizes and functionalities drives the capacity of β CD-tNG to enhance the encapsulation and dermal penetration of hydrophobic molecules.

2. Experimental Section

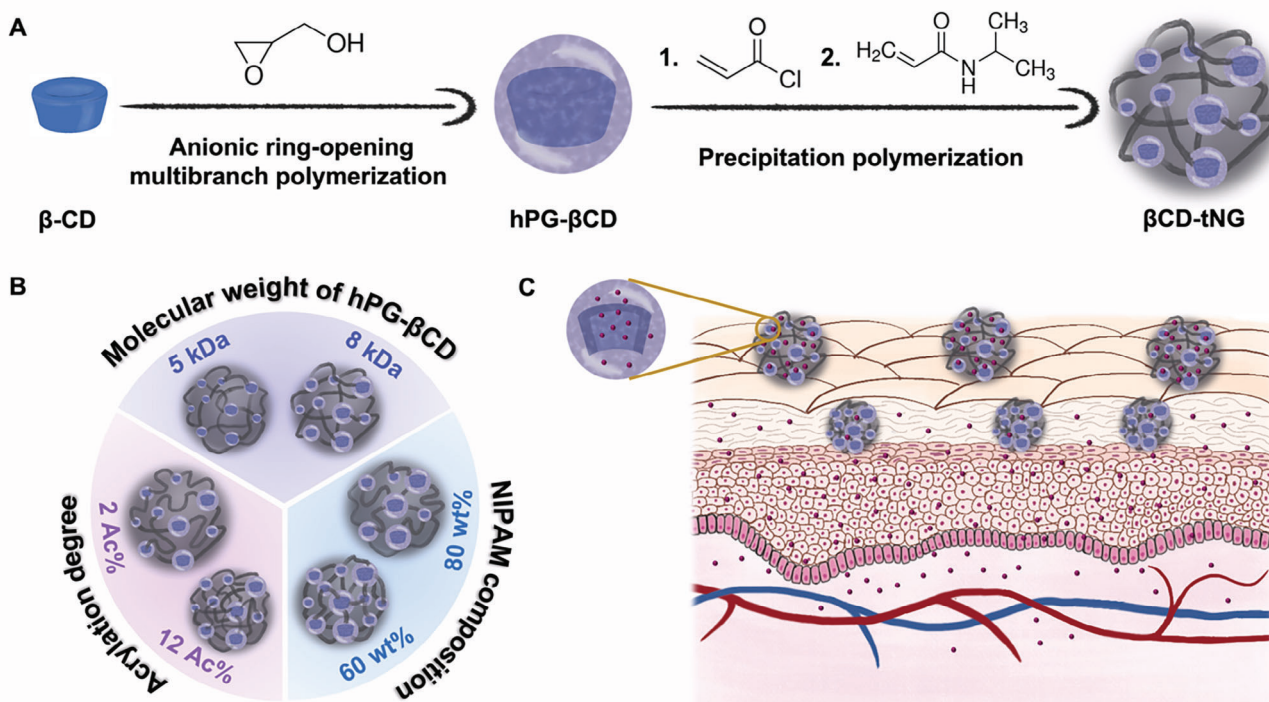
2.1. Materials

β -CD, glycidol, potassium hydride, 18-crown-6, acryloyl chloride, triethylamine, sodium dodecyl sulfate (SDS), potassium persulphate (KPS), NR, and NIPAM were purchased from Sigma Aldrich (Spain). OCT mounting medium, paraformaldehyde, disodium phosphate (Na_2HPO_4), potassium phosphate (KH_2SO_4), NaCl, and KCl were purchased from Scharlab (Spain). All solvents including methanol, dry DMF, and DMSO were purchased from Merck (Spain). Glycidol was dried over activated molecular sieves overnight at room temperature and distilled under a vacuum before use. β -cyclodextrin was recrystallized with deionized water two times followed by drying under vacuum at 60 °C overnight and stored at 4 °C under a nitrogen atmosphere until use. All other reagents were used as purchased unless specifically mentioned.

2.2. Synthetic Methods

2.2.1. Synthesis of Hyperbranched Polyglycerol Modified β -CD

The crosslinker, hPG- β CD, was synthesized using anionic ring-opening multibranch polymerization (ROMBP). For the reaction, β -CD (0.6 g, 0.5 mmol) and 18-crown-6 (0.25 g, 0.94 mmol) were dissolved in 10 mL dry DMF in a 25 mL round-bottomed flask under stirring at room temperature for 1 h. After forming a homogeneous solution, potassium hydride (50 mg, 1.25 mmol) was added to the flask slowly under a nitrogen atmosphere. The mixture was kept under stirring for another 2 h at room temperature to allow the partial deprotonation of β -CD moieties, as shown in Scheme S1 (Supporting Information). Then, glycidol (2.715 mL, 34 mmol) was added dropwise throughout 20 h. The slow addition of monomers was carried out to avoid the formation of homopolymers. After stirring for 20 h at 80 °C with nitrogen protection, the mixture was cooled down to room temperature and quenched by dilution to 30 mL. The product was dialyzed by cellulose membrane with molecular weight cut-off (MWCO) of 1 kDa, against distilled water for 3 days by changing the water at frequent time intervals to remove unreacted reagents. It was followed by lyophilization to obtain the final product, hPG- β CD showing a pale-yellow viscous liquid. The hPG- β CD should be stored under an inert atmosphere at –20 °C for further use. HPG- β CD with two different molecular weights was synthesized using different monomer/initiator ratios as indicated in Table S1 (Supporting Information).



Scheme 1. A) Synthetic methodology of β CD-tNGs, following the hPG-functionalization of β -CD, the acrylation of hPG- β CD, and precipitation polymerization with NIPAM. B) The studied synthetic parameters, including the molecular weight and acylation degree of the hPG- β CD, and the NIPAM composition in the β CD-tNGs, for comprehensively understanding their corresponding effects on dermal penetration of hydrophobic molecules. C) Schematic illustration of Nile Red dermal penetration with the aid of β CD-tNGs.

2.2.2. Synthesis of Acrylated hPG- β CD

For the further formation of pNIPAM-based tNGs, the as-prepared hPG- β CD needs to be acrylated to be the macro-crosslinker, as shown in Scheme S2 (Supporting Information). First, β -CD (500 mg, 6.75 mmol) was dissolved in 10 mL dry DMF under sonication for 10 min. It was followed by the addition of triethylamine (0.15 mL) in an inert atmosphere using the syringe, and cooling down to 0 °C in an ice bath under stirring. Then a certain amount of acryloyl chloride was added dropwise, as indicated in Table S2 (Supporting Information). Afterward, the reaction was processed at room temperature overnight with protection from light. To remove unreacted acryloyl chloride and obtain the purified product, the reaction mixture was dialyzed in a dialysis membrane (MWCO = 1 kDa) against methanol. After 24 h in methanol, the dialysis was continued for another 2 days in deionized water with changing the water at frequent time intervals. The final purified product was stored as an aqueous solution (20 mg mL⁻¹) in an amber vial covered by aluminum foil at 4 °C until further use.

2.2.3. Synthesis of the β CD-tNGs

The β CD-tNGs were synthesized according to previously reported methods (Scheme S3, Supporting Information).^[39] Briefly, for the synthesis of β CD-tNGs, acrylated hPG- β CD (30 mg), NIPAM (70 mg), and SDS (2 mg) were dissolved in

Table 1. Composition of various synthesized β CD-tNGs.

Sample's name	Mw of hPG- β CD (Da) ¹	Acylation degree of total OH groups ²	NIPAM / hPG- β CD ³		
			60/40	70/30	80/20
5k-2A	4918	2.3%	59/41	70/30	77/23
5k-6A		5.7%	58/42	67/33	74/26
5k-12A		13%	68/32	66/24	79/21
8k-2A	8021	2.3%	69/31	73/27	78/22
8k-6A		6.3%	63/37	74/26	80/20
8k-12A		11.4%	73/27	80/20	83/17

★ 1, 2, 3: All the actual molecular weights and acylation degrees of hPG- β CD and the compositions of NIPAM were determined by NMR analysis.

Milli Q water and purged with nitrogen for 30 min. Then, KPS (3.3 mg) was added to the reaction mixture. The reaction was kept under 350 rpm stirring at 70 °C for 3 h and then purified by dialysis against Milli Q water using a dialysis membrane (MWCO = 10 kDa) for 3 days by changing the Milli Q water at frequent time intervals. The final product was lyophilized presenting as fluffy white solid. Various β CD-tNGs were synthesized with different acylation degrees and molecular weights of hPG- β CD and different compositions of NIPAM, as mentioned in Table 1.

2.3. Characterization of β CD-tNGs

2.3.1. Nuclear Magnetic Resonance (NMR) Spectroscopy

The ^1H NMR spectra were collected at 25 °C by Bruker Advance DPX 300 with 300 MHz of resonance frequency, under experimental conditions of 128 scans and 64 s relaxation time. To prepare the solution, 10 mg samples were dispersed in 0.9 mL Milli Q water and mixed with 0.1 mL deuterated water (D_2O) at room temperature prior to the NMR analysis. The spectra were analyzed through MestreNova software.

The molecular weight of synthesized hPG- β CD was calculated according to the signals at $\delta = 5.1, 3.33, 4.1,$ and 4.8 , which correspond to the anomeric proton of β -CD, the four methylene protons and one methane proton of hPG, and the hydroxyl protons, respectively (additional information about the calculation is included in Figure S1, Supporting Information). The acrylation degree of the synthesized hPG- β CD crosslinker was calculated according to the ratio of the signals at $\delta = 5.1$ and $5.8 - 6.4$, corresponding to the anomeric proton of β -CD and the vinyl protons after acrylation, respectively. The ratio of pNIPAM in the β CD-tNGs to hPG- β CD was calculated as a percentage of the ratio of the signals at $\delta = 3.25 - 4.25$ from the β -CD moieties and $\delta = 0.5 - 2.5$ from the 9 protons of pNIPAM moieties.

The ^{13}C NMR spectra were measured at 25 °C and 300 MHz of resonance frequency using a Bruker Advance DPX Bruker BioSpin Fourier 300 NMR, under experimental conditions of 12 288 scans, relaxation delay of 1.5 s, and acquisition time of 1.73 s. The samples were prepared at 20 mg mL^{-1} of concentration in D_2O as solvent.

2.3.2. Dynamic Light Scattering (DLS)

The hydrodynamic diameters and zeta potential of β CD-tNGs were determined by DLS and electrophoretic mobility, respectively, using a Malvern NanoZS Zetasizer. All the β CD-tNGs samples were measured as aqueous solution with a concentration of 1 mg mL^{-1} and polystyrene was chosen to be the standard. After equilibrium of 60 s, the corresponding hydrodynamic diameters and polydispersity index (PDI) at 25 °C were recorded according to the intensity distribution. The zeta potentials of the samples were measured at pH 7 and 25 °C after equilibrium of 60 s.

2.3.3. Thermo-responsive Performance Determined by Measuring the T_{cp}

Above the transition temperature, thermo-responsive β CD-tNGs undergo decreased hydrodynamic sizes and hydrophilicity, showing a turbid change of the dispersion, which alters their UV-Vis absorbance. In consequence, the T_{cp} was analyzed through UV-vis absorbance using a microplate reader equipped with a temperature-controlled system. Various NGs were dispersed in MilliQ water to form clear dispersions (1 mg mL^{-1}). The experiment was carried out at a temperature range of 26 – 52 °C, with a heating gradient of 1 °C. At each temperature point, the plate was shaken orbitally for 5 min, delayed for 3 min, and further orbitally shaken for 5 min before reading the spectra, to reach a

temperature equilibrium in the tNGs dispersion. The transmittance of β CD-tNGs samples was obtained via a calculation based on the absorbance at 600 nm following the equation below:

$$\text{Transmittance\%} = 10^{2 - \text{Absorbance}} \quad (1)$$

2.3.4. Atomic Force Microscopy (AFM) Imaging

AFM measurements were performed on AFM Dimension ICON (Bruker) equipped with a cantilever ScanAsyst (Bruker) (70 kHz, 0.4 N/m) at room temperature in PeakForce Tapping mode. 5 μL NGs aqueous solutions (0.02 mg mL^{-1}) were deposited onto the freshly cleaved mica substrate. The substrates were incubated overnight at room temperature to evaporate the moisture. Before the measurement, cantilevers needed to be calibrated on a Sapphire substrate. To perform the characterization, the substrate was mounted on a magnetic platform. It was followed by the PeakForce Tapping scanning with 512 points per line and a rate of 0.9 Hz. Image analysis was programmed by NanoScope Analysis. All the images should be flattened in 3rd order to correct the defect generated by the scanning process.

2.4. Encapsulation of NR into β CD-tNGs

To encapsulate NR within β CD-tNGs, lyophilized NGs were re-dispersed in 0.5 mL PBS solution (10 mM, pH 7.4) to reach a concentration of 2 mg mL^{-1} . Then, 75 μL methanol NR stock solution ($c = 1$ mg mL^{-1}) was added into the NGs dispersion (NGs/NR mass ratio = 13.3) and mildly shaken overnight at 37 °C in darkness. Afterward, the mixture was intensively shaken for 1 h at 60 °C with the cap opened to evaporate MeOH. Finally, the NR loaded-NGs dispersion was kept in the fridge at 4 °C to allow the tNGs re-dispersing in the solution. After overnight incubation, unloaded NR was removed by filtration using a filter paper disk with 5–8 μm particle retention. Since hydrophobic NR molecules can form precipitation in an aqueous solution, they can not pass the filter paper along with the hydrophilic tNGs. To evaluate the amount of loaded NR molecules, the NR-loaded tNGs were lyophilized, then 1 mL ethyl acetate was added to the lyophilized NR-loaded β CD-tNGs to extract the loaded NR. The loaded NR was quantified by UV-Vis using an NR calibration curve in ethyl acetate as the reference. Confirmation of NR within the β CD-tNGs is discussed in detail in Section 4 of the supporting information section.

The equation to calculate the encapsulation capacity is shown as:

$$\text{Encapsulation efficiency (\%)} = \frac{m_{\text{encapsulated NR}}}{m_{\text{initial NR}}} \quad (2)$$

2.5. Quantitative Analysis of NR Dermal Penetration

The porcine thigh skin were freshly obtained from a local butcher. The fresh skin was cleaned by removing the fat layer and washing the surface carefully. To mimic the pathological skin condition, tape-stripping was applied 70 times to damage the stratum

corneum. Square skin pieces of 1 × 1 cm were cut, quickly frozen in liquid nitrogen, and stored in the freezer at −20 °C. Before using, the frozen skin pieces were put on the PBS-wetted cotton in a Petri dish to defrost at 4 °C overnight.

To perform the dermal penetration assays, the skin pieces were placed on a new Petri dish with wet cotton on the bottom to prevent skin dehydration. Then, 50 μL of NR-loaded tNGs prepared following the above-mentioned procedure was added onto the skin surface and incubated for 6 h to evaluate NR dermal penetration. To get close to the real scenario of skin penetration, the incubation temperature was increased from 32 °C to 37 °C at a speed of 1 °C per 30 min to mimic the temperature gradient along the skin layers and kept at 37 °C for another 3.5 h.

Finishing the incubation, the skin pieces were rinsed with PBS solution (10 mM, pH 7.4), and the unpenetrated NR was carefully removed using a soft napkin. Afterward, the treated skin samples were scratched by a scalpel, and placed into 1 mL ethyl acetate separately. To fully extract the penetrated NR, the skin samples were further incubated in ethyl acetate for at least 24 h after a 10-min sonication. Moreover, another 10-min sonication was employed before the measurement to ensure complete NR extraction. The penetrated NR was quantified by UV-vis spectrophotometer using an NR calibration curve in ethyl acetate as the reference, and the results were informed as the mass of penetrated NR per skin area. Each sample was performed at least in triplicates.

2.6. Analysis of Dermal Penetration Depth of NR by Fluorescence Microscopy

The dermal penetration depth of NR was investigated with an inverted epifluorescence microscope (Cell Observer Zeiss). First, the skin pieces were incubated in a process that is the same as the skin penetration study above. After completing the incubation, each skin piece was fixed in 4% paraformaldehyde at 4 °C for 48–72 h after cleaning the surface. Then, the skin samples were carefully washed with distilled water, and sunk into 1% sucrose solution for 24 h and another 24 h with 30% sucrose solution at 4 °C. Whereafter, the skin pieces were cleaned and embedded into OCT mounting medium for further freezing. The cryosections of 20 μm were obtained using a Cryostat CM 3050 S from Leica Biosystems (Nussloch, Germany). The operation was processed in a chamber of −30 °C. The images were analyzed using ImageJ software.

2.7. Skin Hydration Studies

Skin pieces of 2×2 cm were quickly frozen in liquid nitrogen after being cleaned and stored in the freezer at −20 °C and defrosted on demand. Before processing the assay, the frozen skin pieces were defrosted overnight at 4 °C in the petri dish with wet cotton on the bottom to keep the skin hydrated. To evaluate the skin hydration effect resulting from the tNGs, the skin pieces were placed between the donor and acceptor compartment of a Franz-cells system, as shown in Scheme S4 (Supporting Information). The receptor compartment was filled with PBS (10 mM, pH 7.4), and each cell was connected to a circulation bath to maintain a stable incubation temperature. The tNGs dispersions in

PBS (10 mM, pH 7.4) were added to the donor compartment and the systems were incubated at 37 °C for 3 h. Subsequently, the skin pieces were taken out and wiped with a soft napkin to remove the free water on the surface. The weight of the treated skin pieces was recorded before and immediately after the incubation, to evaluate the increase in water content after the treatment with tNGs. The experiments were performed with 10 times replications.

2.8. Statistical Analysis

All the skin assays were performed at least in triplicate. The results were shown as the mean value ± SD. They were analyzed by two-way ANOVA with Bonferroni post-test analysis. *P* values * < 0.05, ** < 0.01, and *** < 0.001 were considered significant in all analyses.

3. Results and Discussion

3.1. Synthesis and Characterization of the βCD-Modified tNGs

Hydrophobic drugs have been widely used in clinics, although they have inferior stability, low aqueous solubility, off-target effects, and high immunogenic potential. To overcome such shortcomings, nanotechnology has been explored for encapsulating them into hydrophilic nanocarriers.^[40,41] However, the lack of miscibility reduces encapsulation efficiency and even leads to precipitation, limiting the clinical application and reducing the drug efficacy. Hence, we were motivated to develop pNIPAM-based tNG with β-CD modification, allowing hydrophobic drugs to get loaded into the cavity of β-CD and improve their overall performance, particularly in dermal drug delivery.

Considering the proper cavity size, availability, and FDA approval, β-CD was employed to be the core to fabricate the crosslinkers for further synthesizing tNG. To improve its biocompatibility and water solubility, β-CD was functionalized by hyperbranched polyglycerol via anionic ring-opening multi-branching polymerization (Scheme S1, Supporting Information).^[42] Then, a partial acrylation of the hydroxy groups of hPG was performed prior to the βCD-tNG synthesis (Scheme S2, Supporting Information). Defined by ¹H-NMR, ¹³C-NMR spectra and GPC spectra, various hPG-βCDs with molecular weights of 5 kDa and 8 kDa (Figures S1–S3, Supporting Information), as well as different acrylation degrees of 2%, 6%, and 12% (Figure S4, Supporting Information), were fabricated. The corresponding synthetic details are shown in Tables S1 and S2 (Supporting Information). Afterward, the βCD-tNGs were prepared via precipitation polymerization^[43] in an aqueous solution at 70 °C using NIPAM as the monomer (Scheme 1; Scheme S3, Supporting Information). As a significant constitution of the tNGs, the compositions of NIPAM monomer were designed as 60%, 70%, and 80% (Figures S5 and S6, Supporting Information) for exploring their differential effect on dermal drug delivery, since pNIPAM could lead to skin hydration effects to promote dermal drug delivery.^[23] All in all, the molecular weight and acrylation degree of the crosslinker and the composition of the monomers were taken into consideration, to investigate the effect of synthetic parameters on skin drug delivery more comprehensively.

Indeed, the structure of NGs is determined by many synthetic parameters, showing different densities of the crosslinked network. The hydrodynamic sizes of β CD-tNGs from different synthetic conditions were analyzed by DLS (Figure 1A), and the corresponding details are presented in Table S3 (Supporting Information). It was found that the molecular weight of hPG- β CD does not have a significant influence on the sizes of the β CD-tNGs in aqueous medium, but the acrylation degree of hPG- β CD and the composition of NIPAM do. While the composition of NIPAM the acrylation degree of hPG- β CD presented opposite influence. Figure 1A illustrates that the increase of hPG- β CD acrylation degree caused a drop in hydrodynamic diameter, for example, from 166.6 ± 3 nm to 92.03 ± 0.8 nm for the β CD-tNGs of 5k-2A-60 and 5k-6A-60, respectively. It might be because the higher acrylation degree of the hPG- β CD can offer more carbon double bonds for subsequent polymerization and crosslinking, which contributes to a more compact polymer network and decreased hydrated diameters. Interestingly, the effect of the acrylation degree of hPG- β CD seems to have a tendency of saturation when it is up to 6%, showing similar hydrodynamic diameters with 6% and 12% acrylation degrees. This might result from the increase of the hydrophobicity of hPG- β CD when the acrylation degree increases. Previous studies from our group have demonstrated that the acrylation degree of hPG-based crosslinkers plays a key role in the stabilization of aggregates during the tNG synthesis.^[39] In a window range of acrylation degrees, acrylated hPG- β CD could stabilize the growing tNGs, leading to smaller particle sizes as the acrylation degrees increased. However, as the acrylation degree increases over the effect window, the crosslinker becomes more hydrophobic causing less efficient stabilization for the NGs during the synthesis, which explains the small changes in sizes obtained for NGs using hPG- β CD with 6% and 12% acrylation degree.^[39] Regarding the effect of NIPAM, the hydrodynamic diameter rises as the composition of NIPAM increases, such as from 92.03 ± 0.8 nm to 269.3 ± 1.4 nm for 5k-6A-60 and 5k-6A-80 β CD-tNGs respectively, on account of the looser crosslinking networks. The zeta potential values for all the β CD-tNGs are slightly negative, with values ranging between -1.5 to -2.5 mV. In view of the thermo-responsiveness, the shrinkage behavior of β CD-tNGs over the transition temperature was also characterized by DLS. Figure 1B presents the swelling ratio of various β CD-tNGs in an aqueous medium, calculated via the ratio of hydrodynamic volumes at 25 °C and 55 °C. Different from hydrodynamic diameters, the molecular weight of hPG- β CD affected the swelling ratio, which was higher for 8k-hPG- β CD samples. HPG- β CD of higher molecular weight can probably give higher flexibility and hydrophilicity to β CD-tNGs leading to higher swelling capacity. In addition, higher acrylation degree of hPG- β CD reduced the swelling ratio without a saturated tendency, which is different from its effect on hydrodynamic diameters. It could be explained as the acrylation degree of hPG- β CD plays a significant role in the density of the network, which directly determines the stiffness and flexibility of β CD-tNGs. Similarly, the higher composition of NIPAM monomer can generate flexible networks with fewer crosslinking points, which presents a higher swelling ratio. Furthermore, the successful formation of β CD-tNGs and their corresponding sizes can be clearly confirmed with the aid of AFM analysis, as shown in Figure 1C. The spherical morphology is easily observed via AFM images, for example, tNGs of 5k-2A-60 and

8k-6A-70, with average de-hydrated diameters of 74 ± 7 nm and 69 ± 6 nm, respectively.

Since the skin possesses a natural temperature gradient ranging from 32 °C on the surface to 37 °C in the inner skin layers, tNGs with the fitting transition temperature are ideal to achieve controllable drug delivery. Then, it is possible to trigger drug release spontaneously upon penetration of the tNGs into the skin. Table S4 (Supporting Information) presents the T_{cp} of various synthesized β CD-tNGs, and the corresponding normalized transition curves are shown in Figure S7 (Supporting Information). Interestingly, herein all β CD-tNGs showed a T_{cp} of around 36 °C, which is slightly higher than the T_{cp} of pNIPAM (32 °C) probably because of the introduction of hydrophilic hPG- β CD macromolecules. It has been reported that different monomers and the hydrophilicity of the NGs affect the transition behavior based on the intensity of the hydrogen bond among the NGs and the water molecules.^[44] Above the T_{cp} , pNIPAM-based tNGs undergo a reversible phase transition, and water molecules are simultaneously expelled. Therefore, the stronger the intrinsic hydrogen bonding interaction between tNGs and water molecules, the higher the T_{cp} . Although all β CD-tNGs showed higher T_{cp} than pNIPAM, the different synthetic parameters (NIPAM content, acrylation degree, and molecular weight of the crosslinker) did not show to affect the hydrogen bonding interaction between β CD-tNGs and water molecules.^[45] Previously, our group reported the synthesis of hPG-NIPAM tNGs decorated with β -CD which showed a T_{cp} of 32.3 °C, similar to undecorated control tNGs (34 °C).^[34] The slight decrease in T_{cp} with respect to the tNGs without β -CD decoration resulted from the surface attaching of β -CD on tNGs. Herein, we introduce a novel synthetic strategy to include the β CD units inside tNGs by synthesizing a hydrophilic crosslinker containing β -CD units as a core. In this way, the hydrophilic crosslinker increases the T_{cp} of tNGs to close to the body temperature, making them even more suitable for dermal delivery applications by avoiding drug release in undesired areas.

3.2. Encapsulation of a Hydrophobic Cargo into Hydrophilic Nanogels

To conquer the obstacle of encapsulating hydrophobic drugs into hydrophilic tNGs, β -CD was incorporated into hydrophilic tNGs to improve their loading capacity of hydrophobic molecules. Herein, NR was selected as the hydrophobic model cargo. Previous studies have verified that β -CD enables the prevention of NR aggregation by exploiting its hydrophobic cavity to load monomeric NR molecules.^[46] In the aqueous solution, NR shows inferior solubility and stability, resulting in broad UV-vis absorption and even an attenuation of absorbance intensity at $\lambda = 580$ nm over time, as well as a widened absorbance peak (Figure S8, Supporting Information). Figure S9 (Supporting Information) portrays the narrowed absorption peak of NR dissolved in a β -CD solution with different concentrations, demonstrating the formation of an inclusion complex between NR and β -CD, and the enhanced solubility up to 5 mM.

To weaken the immiscibility between the β CD-tNGs and NR, an overnight incubation at 40 °C was applied in the loading process. Due to their decreased hydrophilicity under high

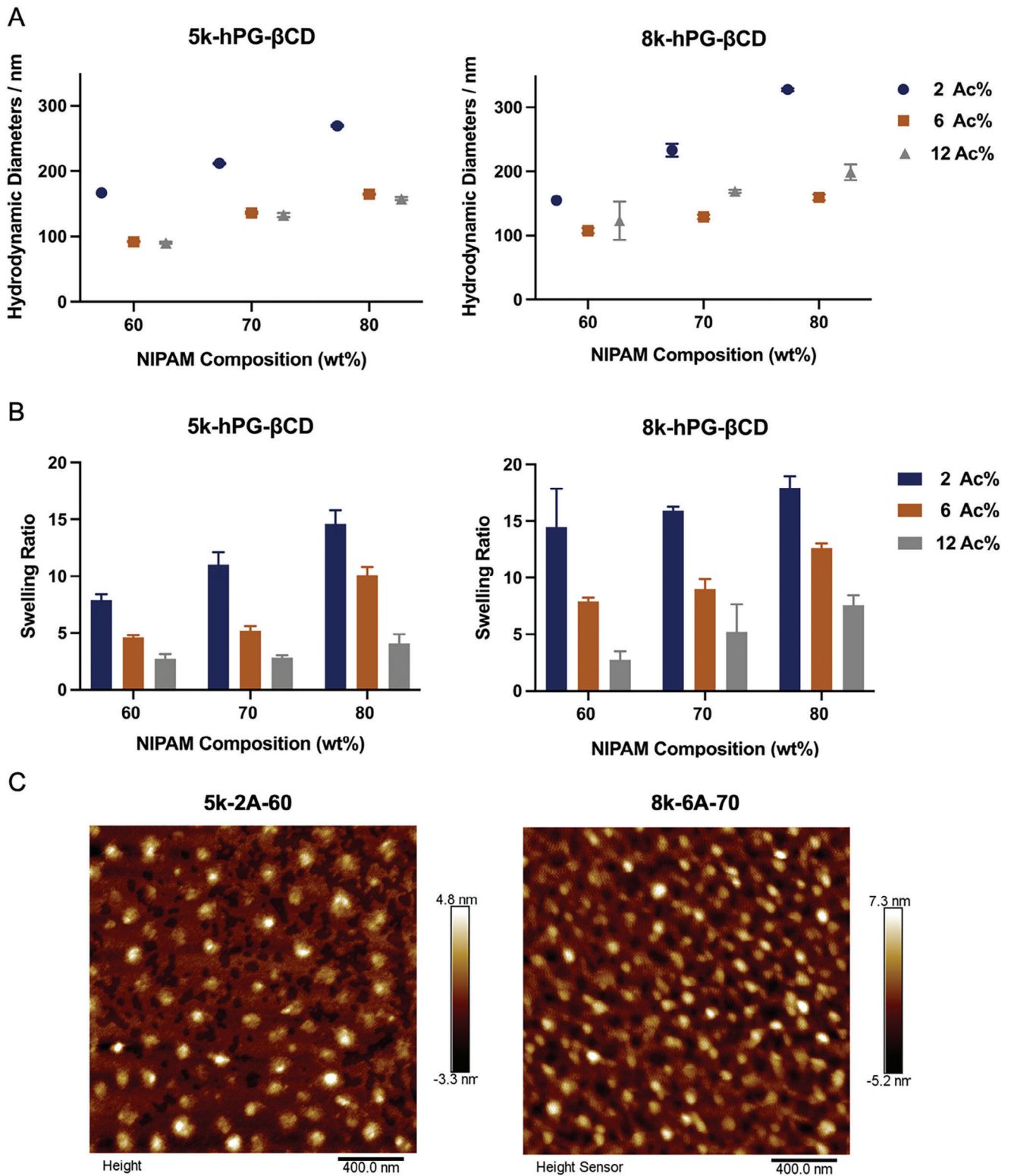


Figure 1. A) Hydrodynamic diameters of various β CD-tNGs obtained from DLS measurement. B) The swelling ratio of various β CD-tNGs, calculated as the variation in size at 25 °C and 55 °C. C) AFM images of β CD-tNGs (5k-2A-60 and 8k-6A-70) with different acrylation degrees and molecular weights of hPG- β CD, and different NIPAM compositions.

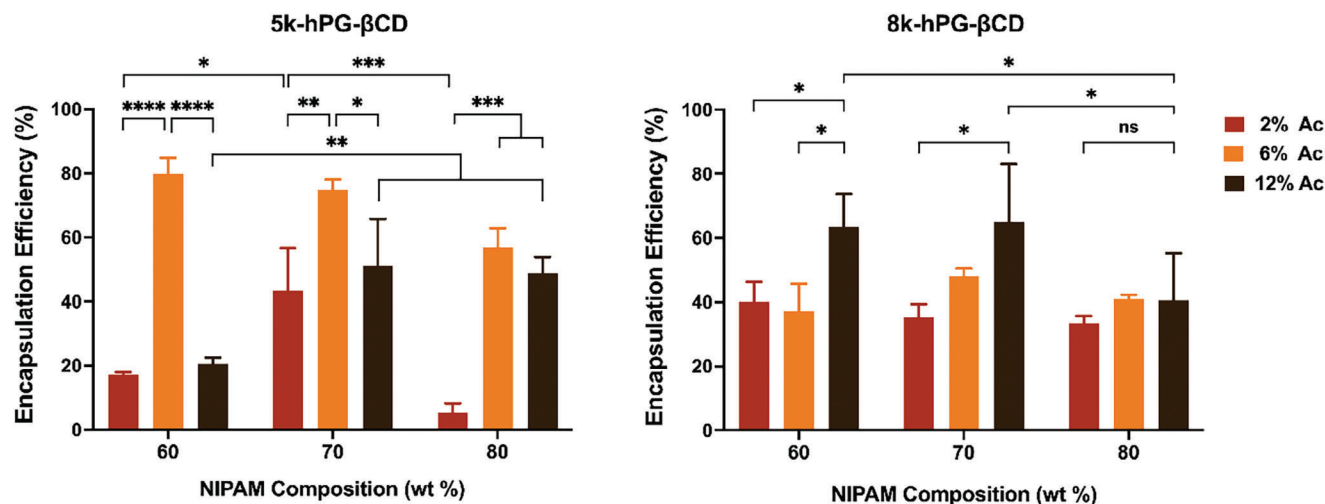


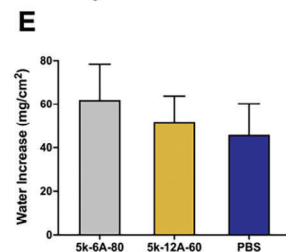
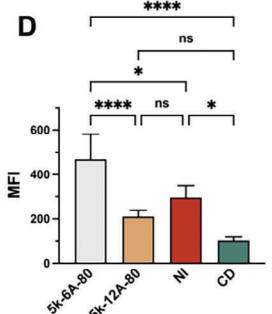
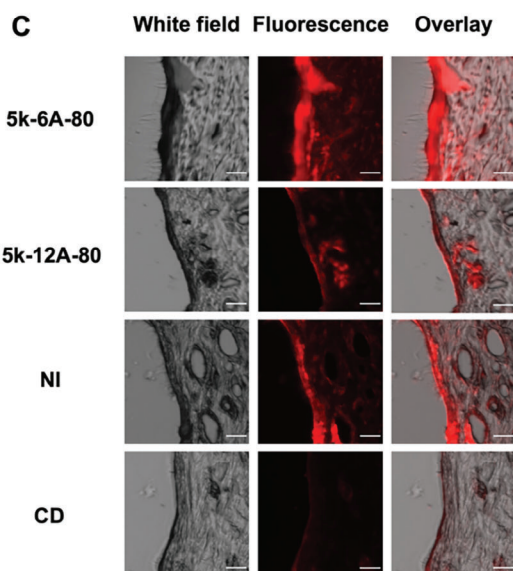
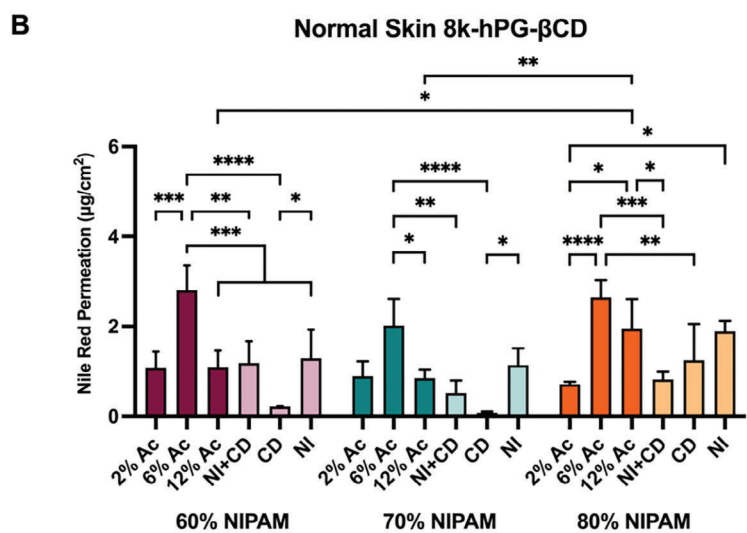
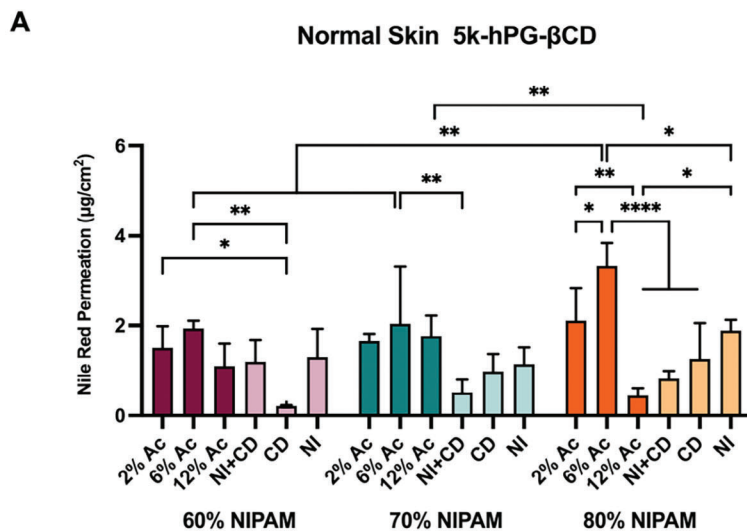
Figure 2. Encapsulation efficiency of NR into various β CD-tNGs, determined by UV-vis spectrophotometry. The NR was encapsulated into the β CD-tNGs at 37 °C for overnight with triplicate. And the UV-vis spectra were collected at room temperature.

temperature, β CD-tNGs exhibited an improved ability to capture NR molecules compared to the condition at 4 °C. As shown in **Figure 2**, most of the β CD-tNGs possessed desirable NR loading efficiency (> 30%). Compared to its poor solubility in water (< 1 $\mu\text{g mL}^{-1}$),^[47] NR obtained increased solubility values up to 120 $\mu\text{g mL}^{-1}$ upon encapsulation in β CD-tNGs. It was observed that the molecular weight of hPG- β CD did not have an obvious effect on the NR loading, while the acrylation degree of hPG- β CD did. For example, for the β CD-tNGs with 5k-hPG- β CD, NR loading efficiency was observed to have a non-linear relationship with the acrylation degree of the crosslinker, which shows a positive correlation with acrylation degree from 2% to 6%, while a negative correlation from 6% to 12%. Whereas, for the β CD-tNGs with 8k-hPG- β CD, NR loading efficiency carried an increased trend with an increased acrylation degree of hPG- β CD, achieving the highest value at 12% acrylation degree. The differential effect from acrylation degree might arise from the distinct hydrophilicity and flexibility of β CD-tNGs crosslinked by hPG- β CD with molecular weights of 5 kDa and 8 kDa. Generally, a higher acrylation degree resulted in a more compact polymer network, which enables the decrease of the water content inside of the tNGs structure and enhances the interaction among β -CD moieties. Apparently, this seems to be beneficial to capture a higher amount of NR molecules into the β CD-tNGs network. Besides, a higher acrylation degree brings lower hydrophilicity, which increases the affinity to NR.^[39] These effects are particularly notable when using macromolecular crosslinkers with higher molecular weight, like 8 kDa. Whereas, with a smaller crosslinker, an excessively higher acrylation degree tends to reduce the loading capacity because of the too compact polymeric network. Regarding the composition of NIPAM in β CD-tNGs, it only has a slight correlation with loading ability. High NIPAM composition increases the hydrophilicity of the β CD-tNGs and results in a looser polymeric network, and yet too low NIPAM composition leads to a compact polymer network. Both are disadvantageous to load NR molecules. Besides, a higher amount of NIPAM content enabled the generation of more hydrophobic space for capturing NR at a temperature above T_{cp} . As a result, the β CD-tNGs with 70 wt%

NIPAM showed relatively good capacity for loading NR in comparison to the β CD-tNGs with 60 wt% and 80 wt% NIPAM.

3.3. NR Dermal Penetration with the Aid of β CD-tNGs

As NR molecules are hydrophobic, they are unlikely to be released into aqueous media. Besides, the traditional methods for in-vitro drug release studies are not suitable for mimicking the real scenario of dermal drug penetration. Hence, to investigate the promotion of β CD-tNGs on NR dermal penetration, a quantitative *ex-vivo* penetration study was performed on porcine skin, under an incubation condition of temperature gradient 32 – 37 °C. Based on our hypothesis, the structure of β CD-tNGs and their ability to facilitate dermal penetration of NR are primarily influenced by the molecular weight and acrylation degree of the hPG- β CD, as well as the NIPAM composition. **Figure 3A,B** comparatively show the amount (μg) of NR that penetrated the skin per square centimeter. The control groups included β -CD, hPG-NIPAM-tNGs, and a physical mixture thereof. In general, the as-prepared β CD-tNGs showed a higher dermal penetration amount of NR compared to the control groups. Especially, the β CD-tNGs 5k-6A-80 showed the highest amount of NR dermal penetration at 3.33 $\mu\text{g cm}^{-2}$ (10.47 nmol cm^{-2}), while 5k-12A-80 showed the lowest 0.44 $\mu\text{g cm}^{-2}$ (1.38 nmol cm^{-2}), which is dramatically higher than other studies for dermal penetration of hydrophobic molecules (1.2 nmol cm^{-2}).^[48] The obvious distinction implies the important role of the crosslinker hPG- β CD on NR dermal penetration. A significantly higher NR penetration was observed in all the tNG samples with hPG- β CD of 6% acrylation degree, compared to the ones with hPG- β CD in 2% and 12% acrylation degree. As mentioned above, the diversity of acrylation degree of hPG- β CD offers differential softness and hydrophilicity to the synthesized β CD-tNGs, which cause inverse effects on the dermal penetration behavior. For instance, β CD-tNGs with the same composition of NIPAM but crosslinker with higher acrylation are supposed to have a more compact and less hydrophilic network, by virtue of providing more active points for



polymerization at each crosslinker and hydrophobicity from the hPG- β CD acrylation. Generally, less hydrophilicity of the tNGs serves dermal drug penetration behavior on account of the skin lipid, but a more compact network goes against drug release behavior due to the lower flexibility. Other than softness, a compact network potentially decreases the capacity of the β CD-tNGs to absorb water and swell. This might comparatively reduce the skin hydration effect, further decrease the skin drug penetration. Given the inverse contribution to the dermal penetration of hydrophobic molecules, there should be a balance between softness and hydrophilicity to achieve desirable dermal penetration. In addition, when the acrylation degree of hPG- β CD was too high at 12%, the crosslinker hPG- β CD was surrounded by a more condensed polymer network, hindering the β -CD extracting lipid from the skin for promoting dermal drug delivery. Therefore, it was considered to be another significant reason for explaining the decreased NR dermal drug delivery when the acrylation degree of hPG- β CD is 12%.

To assess the improvement of NR dermal penetration depth from as-prepared β CD-tNGs, β CD-tNGs of 5k-6A-80 and 5k-12A-80 were selected to be analyzed by epifluorescence microscopy, compared with β -CD solution and the tNG without β -CD (NI), as shown in Figure 3C. Through analyzing the mean fluorescent intensity (Figure 3D), it was found that the β -CD solution presented only a weak fluorescent signal from NR inside the skin. This result suggests that β -CD alone did not possess significant promotion for NR dermal penetration. Nevertheless, the tNGs (80-NI, 5k-6A-80, and 5k-12A-80) showed prominent enhancement in the dermal penetration of NR, as evidenced by their stronger fluorescent signal. Thereinto, the NR penetration promoted by 5k-6A-80 β CD-tNGs showed to be comparatively greater, in terms of the fluorescent intensity and the penetration depth, highlighting that the introduction of hPG- β CD into tNGs as crosslinkers facilitates the dermal penetration of hydrophobic molecules. Interestingly, a chemically equivalent control 80-NI tNG without β -CD, presented a lower NR penetration amount than 5k-6A-80, but higher than 5k-12A-80, hinting at an evident influence of acrylated crosslinker hPG- β CD on NR dermal penetration. It proves our hypothesis that excessive acrylation of hPG- β CD might generate a negative influence on the penetration behavior due to the reduced flexibility of the β CD-tNGs and concealing of the β -CD moieties.

In addition to the acrylation degree of hPG- β CD, the composition of NIPAM was shown to slightly influence the NR dermal penetration as well. Via the statistical analysis, it was observed that the β CD-tNGs with 80% NIPAM composition exhibited comparable higher dermal penetration than the ones with 60% and 70% NIPAM composition. It has been reported that softer NGs can better fit the protein/lipid structure in the SC, and interact with it, contributing to more efficient dermal drug

penetration.^[49] Another consequence of higher NIPAM composition is higher absorption of water in the β CD-tNGs, which consequently induces a higher hydration effect on the skin, promoting the dermal penetration of therapeutic molecules. The hydration effect is a reversible and non-invasive process to the skin structure that improves skin condition. It can also enhance skin permeability to further promote the dermal penetration of therapeutic molecules and improve blood flow to further optimize the dermal absorption of the therapeutic molecules.^[50,51] It has been demonstrated that hPG-NIPAM-based tNGs enable skin hydration and perturbation of the organization of the keratin filaments and lipid lamellae.^[23,24] To verify this hypothesis, the increase of water content after the incubation with β CD-tNGs was quantified using the experimental setup shown in Scheme S4 (Supporting Information). Representative β CD-tNGs, 5k-6A-80 and 5k-12A-60, were selected to detect the differential skin hydration effect compared to PBS buffer. After a 3 h-incubation, the skin sections were visibly hydrated in the area of treatment. In Figure 3E, it can be seen that β CD-tNGs showed slightly higher enhancement of water content than PBS-treated skin sections. Particularly, β CD-tNGs of 5k-6A-80 exhibited comparable superiority in increasing water content inside of the skin structure, which corresponds to the result of the quantitative NR dermal penetration. Despite the differences were not statistically different ($p > 0.05$), considering that the skin hydration effect only happens in the stratum corneum with swollen keratin fiber, we assume that the current distinction is enough to indicate the improved skin hydration effect from β CD-tNGs.^[52,53] It illustrates that the skin hydration effect is also one of the important factors for β CD-tNGs to promote the dermal penetration of NR and explains that a higher proportion of NIPAM monomers benefits the dermal penetration of NR. Overall, with the combination of β -CD and pNIPAM, the designed system exhibited superior capacity in dermal penetration of hydrophobic drugs, based on the possible lipid extraction from β -CD and the skin hydration effect from hPG-pNIPAM based NGs.^[32]

Moreover, to mimic a pathological skin condition, a 70-times tape-stripping was applied to normal skin to damage the SC. The assay of quantitative NR dermal penetration was also processed on tape-stripped skin, evaluating the differential dermal drug penetration capacity of healthy and pathological skin, as shown in Figure S10 (Supporting Information). The tape-stripped skin presents much higher NR penetration efficacy, up to $5.36 \mu\text{g cm}^{-2}$, arising from the damaged defense of the stratum corneum. In another study, a designed chitosan nanosponge enabled the promotion of NR dermal penetration up to $4.5 \mu\text{g cm}^{-2}$, with the free NR penetration only $0.4 \mu\text{g cm}^{-2}$, when the incubation time is at 6 h.^[54] In comparison, our as-prepared β CD-tNGs presented better promotion on NR dermal penetration. The results followed the same trend as the results on normal skin,

Figure 3. Quantitative dermal penetration of NR in porcine skin by means of the β CD-tNGs synthesized with hPG- β CD with a molecular weight of 5 kDa (A) and 8 kDa (B). The β CD-tNGs with various acrylation degrees of the crosslinker hPG- β CD (2%, 6%, and 12%) and the NIPAM composition (60%, 70%, and 80%) were compared with hPG-NIPAM-NGs (NI), β -CD and physical mixture of β -CD and hPG-NIPAM-NGs (NI), to evaluate the corresponding improvement of NR dermal penetration. Statistical analysis was processed by two-way ANOVA method with Bonferroni's multiple comparisons tests (**** $p < 0.0001$, *** $p < 0.001$, ** $p < 0.01$, * $p < 0.05$). C) Fluorescence imaging of skin sections after 6 h-treatment of representative NR encapsulated β CD-tNGs of 5k-6A-80 and 5k-12A-80, NIPAM-NGs, and β -CD solution. Scale bar = 50 μm . D) Analysis of mean fluorescence intensity (MFI) by area of the skin layers. $N = 6$. E) Skin hydration effect of β CD-tNGs 5k-6A-80 and 5k-12A-60, as compared, with PBS after an incubation of 3 h at 37 °C. The mean values were obtained by the replicated experiments ($N = 12$).

regarding the effect of the molecular weight and acrylation degree of hPG- β CD crosslinker and the composition of NIPAM monomer to the dermal penetration of NR. It highlights that our as-prepared β CD-tNGs can effectively promote NR dermal penetration, especially to the pathological skin with damaged SC.

4. Conclusion

In this study, we designed pNIPAM-based tNGs with suitable T_{cp} for dermal drug delivery applications using hPG- β CD as crosslinker. In order to comprehensively investigate their dermal drug delivery capacity, different synthetic parameters, including the molecular weight and acrylation degree of hPG- β CD and the composition of NIPAM monomer, were taken into consideration for synthesizing various β CD-tNGs. Therein, the acrylation degree of hPG- β CD showed to be the main parameter affecting the encapsulation efficiency as well as the dermal penetration of NR, since it defines the softness and hydrophilicity of the β CD-tNGs. The increase of hPG- β CD acrylation degree could reduce the hydrophilicity of β CD-tNGs and thereby facilitate the loading of hydrophobic drugs and the interaction with the SC. When the acrylation degree increases above a certain value, its effect on hydrophilicity would arrive at a saturation plateau, but the stiffness of the β CD-tNGs is still enhanced, which is adverse to drug penetration. Besides, a higher acrylation degree of hPG- β CD results in a more condensed polymer network around the crosslinker hPG- β CD, hindering β -CD's capacity to extract skin lipids to be a penetration enhancer. Whereupon too high acrylation degree of hPG- β CD decreases dermal penetration of NR. Hence, β CD-tNGs with a 6% acrylation degree exhibit higher dermal penetration of NR rather than 2% and 12%. Furthermore, the composition of NIPAM slightly promoted NR dermal penetration efficiency via the skin hydration effect. While the molecular weight did not show an evident effect on dermal drug delivery.

All in all, this study demonstrated that β CD-tNGs can enhance the dermal penetration of hydrophobic model cargo NR, on account of their unique chemical features. On the one hand, the β -CD offers the possibility to load hydrophobic molecules more efficiently by forming inclusion complexes with them. On the other hand, β -CD may enhance skin permeability by lipid extraction to promote the dermal penetration of hydrophobic drugs. Meanwhile, the acrylation degree of the hPG- β CD crosslinker greatly influences the efficiency of hydrophobic drug delivery. This study presents for the first time a systematic investigation of the effect on dermal penetration of hydrophobic drugs based on β -CD-modified tNGs. Although further investigations are needed to address the full potential of this type of tNGs, like a comprehensive assessment of their biocompatibility and their capacity to deliver drugs of high molecular weight, this work lays the first cornerstone towards their application in the treatment of skin diseases.

Supporting Information

Supporting Information is available from the Wiley Online Library or from the author.

Acknowledgements

The authors are thankful to MINECO (RTI2018-098951-B-I00), IKERBASQUE-Basque Foundation for Science, Basque Government

(Elkartek projects KK-2019/00086 and KK-2020/00010; proyectos de investigación básica/aplicada PIBA_2023_1_0043), Gipuzkoa Provincial Council (2019-CIEN-000075-01), LEO Foundation (LF-OC-22-000954), the University of the Basque Country (projects COLLAB22/05 and GIU21/033), and to POLYMAT, Basque Centre for Macromolecular Design and Engineering for funding. H.W. appreciates the financial support received from China Scholarship Council (File no. 201 804 910 606). M.S.O. is thankful for the funding from the European Union's Horizon 2020 research and innovation program under the Marie Skłodowska-Curie grant agreement No 896 775. Dr. Sergio Martin Saldaña, Dr. Krishan Kumar, and Jakes Udabe are acknowledged for proofreading the manuscript and giving scientific inputs. The authors thank the UPV/EHU for technical and human support provided by the SGIker services.

Conflict of Interest

The authors declare no conflict of interest.

Author Contributions

H.W. and N.T. contributed equally to this work. H.W., N.T., M.S.O., and M.C. conceived the idea and project. N.T., L.N., Z.B., and M.A. synthesized and characterized the hPG- β CD crosslinkers. N.T. synthesized and characterized the tNGs by DLS, NMR, and UV-Vis. H.W. characterized the tNG by AFM. H.W. and M.S.O. handled the cloud point temperature characterization and the NR encapsulation, as well as the *in-vitro* skin experiments, including quantitative dermal penetration, fluorescence microscope, and skin hydration. H.W. was in charge of writing this manuscript, while N.T. wrote the section on material synthesis. M.S.O. and M.C. revised and improved the manuscript. M.C. supervised the work and was responsible for funding. All authors have revised and approved the final version of the manuscript. The authors declare that they have no competing interests.

Data Availability Statement

The data that support the findings of this study are available from the corresponding author upon reasonable request.

Keywords

dermal drug delivery, hydrophobic drugs, thermoresponsive nanogels, β -cyclodextrin

Received: December 1, 2023

Revised: March 15, 2024

Published online:

- [1] V. Krishnan, S. Mitragotri, *Adv Drug Deliv Rev* **2020**, *153*, 87.
- [2] M. R. Prausnitz, R. Langer, *Nat. Biotechnol.* **2008**, *26*, 1261.
- [3] A. Z. Alkilani, M. T. C. McCrudden, R. F. Donnelly, *Pharmaceutics* **2015**, *7*, 438.
- [4] R. Langer, *Adv Drug Deliv Rev* **2004**, *56*, 557.
- [5] Y. Q. Yu, X. Yang, X. F. Wu, Y. Bin Fan, *Front Bioeng Biotechnol* **2021**, *9*, 646554.
- [6] M. J. Mitchell, M. M. Billingsley, R. M. Haley, M. E. Wechsler, N. A. Peppas, R. Langer, *Nat Rev Drug Discov* **2021**, *20*, 101.
- [7] M. Lapteva, K. Mondon, M. Möller, R. Gurny, Y. N. Kalia, *Mol Pharm* **2014**, *11*, 2989.
- [8] M. Z. Wang, J. Niu, H. J. Ma, H. A. Dad, H. T. Shao, T. J. Yuan, L. H. Peng, *J. Controlled Release* **2020**, *322*, 95.

- [9] M. Giubudagian, G. Yealland, S. Hönzke, A. Edlich, B. Geisendörfer, B. Kleuser, S. Hedtrich, M. Calderón, *Theranostics* **2018**, *8*, 450.
- [10] F. Rancan, H. Volkmann, M. Giubudagian, F. Schumacher, J. I. Stanko, B. Kleuser, U. Blume-Peytavi, M. Calderón, A. Vogt, *Pharmaceutics* **2019**, *11*, 394.
- [11] F. F. Sahle, M. Giubudagian, J. Bergueiro, J. Lademann, M. Calderón, *Nanoscale* **2017**, *9*, 172.
- [12] T. Subongkot, T. Ngawhirunpat, P. Opanasopit, *Pharmaceutics* **2021**, *13*, 404.
- [13] K. Sudhakar, S. Fuloria, V. Subramaniyan, K. V. Sathasivam, A. K. Azad, S. S. Swain, M. Sekar, S. Karupiah, O. Porwal, A. Sahoo, D. U. Meenakshi, V. K. Sharma, S. Jain, R. N. Charyulu, N. K. Fuloria, *Nanomaterials* **2021**, *11*, 2557.
- [14] Z. Zhao, M. Li, L. Zheng, Y. Yang, X. Cui, T. Xu, W. Zhang, C. Wang, *J. Controlled Release* **2022**, *343*, 43.
- [15] T. S. Anirudhan, S. S. Nair, *Materials Science and Engineering C* **2019**, *102*, 437.
- [16] N. Tiwari, E. R. Osorio-Blanco, A. Sonzogni, D. Esporrín-Ubieto, H. Wang, M. Calderón, *Angewandte Chemie – International Edition* **2022**, *61*, 202107960.
- [17] H. Ragelle, S. Colombo, V. Pourcelle, K. Vanvarenberg, G. Vandermeulen, C. Bouzin, J. Marchand-Brynaert, O. Feron, C. Foged, V. Préat, *J. Controlled Release* **2015**, *211*, 1.
- [18] J. C. Cuggino, M. Molina, S. Wedepohl, C. I. A. Igarzabal, M. Calderón, L. M. Gugliotta, *Eur. Polym. J.* **2016**, *78*, 14.
- [19] K. S. Soni, S. S. Desale, T. K. Bronich, *J. Controlled Release* **2016**, *240*, 109.
- [20] M. Molina, M. Asadian-Birjand, J. Balach, J. Bergueiro, E. Miceli, M. Calderón, *Chem. Soc. Rev.* **2015**, *44*, 6161.
- [21] S. Pawłowska, C. Rinoldi, P. Nakielski, Y. Ziai, O. Urbanek, X. Li, T. A. Kowalewski, B. Ding, F. Pierini, *Adv. Mater. Interfaces* **2020**, *7*, 202000247.
- [22] P. Nakielski, S. Pawłowska, C. Rinoldi, Y. Ziai, L. De Sio, O. Urbanek, K. D. O. I. Zembrzycki, M. Pruchniewski, M. Lanzi, E. Salatelli, A. Calogero, T. A. Kowalewski, A. L. Yarin, F. Pierini, *ACS Appl. Mater. Interfaces* **2020**, *12*, 54328.
- [23] M. Giubudagian, F. Rancan, A. Klossek, K. Yamamoto, J. Jurisch, V. C. Neto, P. Schrade, S. Bachmann, E. Rühl, U. Blume-Peytavi, A. Vogt, M. Calderón, *J. Controlled Release* **2016**, *243*, 323.
- [24] E. R. Osorio-Blanco, F. Rancan, A. Klossek, J. H. Nissen, L. Hoffmann, J. Bergueiro, S. Riedel, A. Vogt, E. Rühl, M. Calderón, *ACS Appl. Mater. Interfaces* **2020**, *12*, 30136.
- [25] B. Chen, B. Wang, W. J. Zhang, G. Zhou, Y. Cao, W. Liu, *Biomaterials* **2012**, *33*, 6086.
- [26] R. Yang, O. S. Okonkwo, D. Zurakowski, D. S. Kohane, *J. Controlled Release* **2018**, *289*, 94.
- [27] B. V. F. Riccio, A. B. Meneguín, F. G. Baveloni, J. A. de Antoni, L. M. G. Robusti, M. P. D. Gremião, P. C. Ferrari, M. Chorilli, *J. Appl. Toxicol.* **2022**, *43*, 1410.
- [28] A. A. Sandilya, U. Natarajan, M. H. Priya, *ACS Omega* **2020**, *5*, 25655.
- [29] X. Zhou, Z. Luo, A. Baidya, H. Jun Kim, C. Wang, X. Jjiang, M. Qu, J. Zhu, L. Ren, F. Vajhadin, P. Tebon, N. Zhang, Y. Xue, Y. Feng, C. Xue, Y. Chen, K. J. Lee, J. Lee, S. Zhang, C. Xu, N. Ashammakhi, S. Ahadian, M. R. Dokmeci, Z. Gu, W. Sun, A. Khademhosseini, *Adv. Healthcare Mater.* **2020**, *9*, 2000527.
- [30] F. Topuz, T. Uyar, *Carbohydr. Polym.* **2022**, *297*, 120033.
- [31] Cyclodextrins as Permeation Enhancers Some Theoretical Evaluations and in Vitro Testing.
- [32] M. V. L. B. Bentley, R. F. Vianna, S. Wilson, J. H. Collett, *J. Pharm. Pharmacol.* **1997**, *49*, 397.
- [33] I. Kritskiy, T. Volkova, T. Sapozhnikova, A. Mazur, P. Tolstoy, I. Terekhova, *Materials Science and Engineering C* **2020**, *111*, 110774.
- [34] M. Giubudagian, S. Hönzke, J. Bergueiro, D. Işık, F. Schumacher, S. Saeidpour, S. B. Lohan, M. C. Meinke, C. Teutloff, M. Schäfer-Korting, G. Yealland, B. Kleuser, S. Hedtrich, M. Calderón, *Nanoscale* **2018**, *10*, 469.
- [35] Z. Zhang, Q. Lv, X. Gao, L. Chen, Y. Cao, S. Yu, C. He, X. Chen, *ACS Appl. Mater. Interfaces* **2015**, *7*, 8404.
- [36] J. Liu, Z. Luo, J. Zhang, T. Luo, J. Zhou, X. Zhao, K. Cai, *Biomaterials* **2016**, *83*, 51.
- [37] S. Abbina, S. Vappala, P. Kumar, E. M. J. Siren, C. C. La, U. Abbasi, D. E. Brooks, J. N. Kizhakkedathu, *J. Mater. Chem. B* **2017**, *5*, 9249.
- [38] M. Witting, M. Molina, K. Obst, R. Plank, K. M. Eckl, H. C. Hennies, M. Calderón, W. Frieß, S. Hedtrich, *Nanomedicine* **2015**, *11*, 1179.
- [39] L. E. Theune, R. Charbaji, M. Kar, S. Wedepohl, S. Hedtrich, M. Calderón, *Materials Science and Engineering C* **2019**, *100*, 141.
- [40] G. Yang, Y. Liu, H. Wang, R. Wilson, Y. Hui, L. Yu, D. Wibowo, C. Zhang, A. K. Whittaker, A. P. J. Middelberg, C. X. Zhao, *Angewandte Chemie – International Edition* **2019**, *58*, 14357.
- [41] J. K. Patra, G. Das, L. F. Fraceto, E. V. R. Campos, M. D. P. Rodriguez-Torres, L. S. Acosta-Torres, L. A. Diaz-Torres, R. Grillo, M. K. Swamy, S. Sharma, S. Habtemariam, H. S. Shin, *J. Nanobiotechnology* **2018**, *16*, 71.
- [42] Z. Xu, Y. Zhang, Q. Hu, Q. Tang, J. Xu, J. Wu, T. B. Kirk, D. Ma, W. Xue, *Materials Science and Engineering C* **2017**, *71*, 965.
- [43] M. Andersson, S. L. Maunu, *J. Polym. Sci. B Polym. Phys* **2006**, *44*, 3305.
- [44] M. Concilio, V. P. Beyer, C. R. Becer, *Polym. Chem.* **2022**, *13*, 6423.
- [45] L. Navarro, L. E. Theune, M. Calderón, *Eur. Polym. J.* **2020**, *124*, 109478.
- [46] A. Ray, S. Das, N. Chattopadhyay, *ACS Omega* **2019**, *4*, 15.
- [47] P. Greenspan, S. D. Fowler, Spectrofluorometric Studies of the Lipid Probe, Nile Red, **1985**.
- [48] P. Dong, F. F. Sahle, S. B. Lohan, S. Saeidpour, S. Albrecht, C. Teutloff, R. Bodmeier, M. Unbehauen, C. Wolff, R. Haag, J. Lademann, A. Patzelt, M. Schäfer-Korting, M. C. Meinke, *J. Controlled Release* **2019**, *295*, 214.
- [49] F. Rancan, M. Asadian-Birjand, S. Dogan, C. Graf, L. Cuellar, S. Lommatzsch, U. Blume-Peytavi, M. Calderón, A. Vogt, *J. Controlled Release* **2016**, *228*, 159.
- [50] J. Petrofsky, G. Bains, M. Prowse, S. Gunda, L. Berk, C. Raju, G. Ethiraju, D. Vanarasa, P. Madani, *J. Med. Eng. Technol.* **2009**, *33*, 532.
- [51] Y. Q. Yu, X. Yang, X. F. Wu, Y. Bin Fan, *Front. Bioeng. Biotechnol.* **2021**, *9*, 646554.
- [52] E. H. Mojumdar, Q. D. Pham, D. Topgaard, E. Sparr, *Sci. Rep.* **2017**, *7*, 15712.
- [53] S. Verdier-Sévrain, F. Bonté, *J. Cosmet. Dermatol.* **2007**, *6*, 75.
- [54] J. S. Lee, H. Oh, S. Kim, J. H. Lee, Y. C. Shin, W. Il Choi, *Pharmaceutics* **2021**, *13*, 1329.